

Proceeding Paper

# A Novel Synthetic Approach of Functionalised GO and CNT to Nanocomposite Containing Active Nanostructured Fillers for Classical Isocyanate Curing <sup>†</sup>

Lina Jadhav <sup>1</sup>, Rahul Patil <sup>1</sup>, Nikhil Borane <sup>1</sup>, Satyendra Mishra<sup>1</sup>, Ganapati D Yadav <sup>2</sup>, Dipak B Patil <sup>3</sup>  
and Vikas Patil <sup>1,2,\*</sup>

<sup>1</sup> University Institute of Chemical Technology, Kavayitri Bahinabai Chaudhari North Maharashtra University, Jalgaon 425001, India; e-mail@e-mail1.com (L.J.); e-mail@e-mail2.com (R.P.); e-mail@e-mail3.com (N.B.); e-mail@e-mail4.com (S.M.)

<sup>2</sup> Institute of Chemical Technology Mumbai, 400019 India; e-mail@e-mail5.com

<sup>3</sup> Universidad de Guanajuato, Campus Guanajuato, División de Ciencias Naturales y Exactas, Departamento de Química, Noria Alta S/N, Guanajuato 36050, Mexico; e-mail@e-mail6.com

\* Correspondence: vikasudct@gmail.com

<sup>†</sup> Presented at the 25th International Electronic Conference on Synthetic Organic Chemistry, 15–30 November 2021; Available online: <https://ecsoc-25.sciforum.net/>.

**Abstract:** A novel synthetic method has been developed by utilizing the chemical reactivity of functionalized graphene and CNT with a covalent combination of chemically diverse GO/FCNT and toluene diisocyanate. Thereby yield a synergistic polymer nanocomposite. Comprehensive composite material has simultaneous covalent as well as  $\pi$ - $\pi$  interactions confirms sp<sup>2</sup>-hybridized frameworks of graphene oxide and MWCNTs by Raman absorption spectra at 1345 and 1590 cm<sup>-1</sup> of D and G band respectively. Toluene diisocyanate and GO/FCNT inspired polymeric formulation obtained by the classical curing reaction initiated by ultrasound sonication. This method allowed 50 wt.% doping of GO/FCNT without segregation ensures good adhesion to the low steel surface. Large surface area and morphological character of GO and FCNT by SEM and TEM ensure stable and dispersed integrated molecules. It has advantages over the high-temperature hazardous curing reaction overcomes the problem of graphene exfoliation and does not allow CNT slipping within the bundle to falls apart at higher concentration.

**Keywords:** graphene; CNT; isocyanate; curing; filler; nanostructured

**Citation:** Jadhav, L.; Patil, R.; Borane, N.; Mishra, S.; Yadav, G.D.; Patil, D.B. A Novel Synthetic Approach of Functionalised GO and CNT to Nanocomposite Containing Active Nanostructured Fillers for Classical Isocyanate Curing. *2021*, *3*, x. <https://doi.org/10.3390/xxxxx>

Academic Editor: Julio A. Seijas

Published: 15 November 2021

**Publisher's Note:** MDPI stays neutral with regard to jurisdictional claims in published maps and institutional affiliations.



**Copyright:** © 2021 by the authors. Submitted for possible open access publication under the terms and conditions of the Creative Commons Attribution (CC BY) license (<https://creativecommons.org/licenses/by/4.0/>).

## 1. Introduction

Complimentary properties of organic and inorganic materials are combined to generate new composite material generating new hybrid composite materials. The new hybrid composite material has combined property of both organic and inorganic compound [1]. Before compositing two chemically distinct species, synergy was installed by functionalisation of an essential component [2]. Functionalization permits chemical response which improves mechanical, thermal, electrical, UV resistance, abrasion properties to hybrid organic-inorganic materials [3,4]. In polymer nano-composite lack of covalent interactions allows exfoliation of filler material into the complex matrix. This problem further overcomes by chemical functionalization and the subsequent covalent combination of nanostructure filler into the polymeric matrix [5]. The isocyanate is ready functional species to be combined with chemically modified filler material thereby enhanced the intrinsic properties of the final composite material for the application. Consequently, the final composite material has reduced hydrophilic properties due to the utilization of hydroxyl and acid functionality of filler and forms new hydrophobic amide and carbamate ester linkage. As a result of this, it is no longer exfoliated into the solvent helps in the stable

dispersed constructive formulation. Segregation has been observed at very low concentration 0.1 vol% of graphene as filler in polystyrene. It was evidenced that there is no constructive attraction between filler and polymer. Physical lying of filler into polymer matrix immediately segregated at high concentration [6,7].

Owing to strong and inbuilt sustainable properties of CNT able to retain 5 to 10 times more load than steel. Comparing to steel CNT inclusion creates magical properties due to the active large surface, 1/6 weight, 50–100 G Pa tensile strength and 1–2 T Pa modulus [8–11]. Next generation performing material lend multifunctionality due to CNT and graphene with unique mechanical, thermal, surface properties. CNT and graphene polymer nanocomposite coating bound synergy of film thickness, the interparticle spacing of the filler and thermomechanical properties [12]. Further 2 wt.% SWNTs addition to coating affects 125% thermal conductivity and 3.5-factor increase Vickers hardness. Still to date the use of CNTs and graphene nanocomposites has been limited by challenges in processing, dispersion, and their prohibitively high cost. Ajayan et al. demonstrated the preparation of epoxy composite by dispersing multiwall nanotubes in the epoxy under the ultrasonic force [13]. Higher concentrations more than 5% nanotubes in composite slip within the bundle and fall apart which is responsible for the poor load transfer within the cured composite. It was supported by Raman spectra, tension and compression analysis [14]. Sandler et al. try to improve dispersion of SWNTs by ultrasonic application and intense stirring. A slight improvement was observed in the configuration of nanotubes still fails on millimeter scale [15]. Irrespective of the sliding of the SWNTs into the ropes continuous increase in Young's modulus was observed with respect to increasing concentration. Improperly configuration slide SWNTs into the ropes and bending of the rope decreases mechanical strength [16]. Furthermore, surfactants were also used to improve the dispersion of nanotubes in epoxy. It retained the mechanical strength of the composition [17]. Surfactant and ultrasonically dispersed epoxy-nanotubes composition appear to be a finely dispersed but microscopic analysis found it to be an inhomogeneous dispersion in the composition [18]. To overcome this; an integrated system is developed upon functionalization of GO/FCNT and exploited to induce curing of diisocyanate. The composite was used as corrosion resistive coating on low alloy steel [19,20]. Loading of 50 wt.% filler achieved stable, mechanically strong and highly dispersed FCNT/GO isocyanate composite for surface coating [21,22].

## 2. Experimental

### 2.1. Materials and Methods

Single-walled carbon nano tubes were purchased from Alfa Aesar. Graphene and toluene diisocyanate precursor was purchased from Sigma Aldrich. Anhydrous THF was used as a solvent in this process and functionalization was done by using  $\text{NaNO}_3$ ,  $\text{KMnO}_4$ , and  $\text{H}_2\text{SO}_4$  in deionized water. Low alloy steel for coating was used from a local supplier, Mumbai, India. Functionalization of CNT and Graphene was performed by the Hummer's method [23]. Further composites were prepared and obtained its fine dispersion. Surface coating of nano-composite on low-alloy steel was performed by simple bar coating method. Formulations contained 50, 25, 10, 5 wt.% of filler content average precise film thickness was obtained.

### 2.2. Characterization of Structure and Surface Morphology

IRRA (infrared reflection absorption) spectra were utilized for the characterization of functional modification in CNT and graphene. IRRA was carried out by Perkin Elmer 100 FT-IR spectrophotometer with Olympus BX51 microscope attachment. Raman spectroscopy was performed by Horiba Jobin Yvon Labram HR system with 514.5 nm laser excitation. The surface morphology of composites were investigated by scanning electron microscopy (SEM) on a Hitachi SU-70 instruments operated at an accelerating voltage of 20 kV. The transmission electron microscopy (TEM) was used for dispersion study of the

composite by a JEOL-2010 instrument operated at 200 kV and 100 mA equipment. Film thickness was measured by shin equipment Mumbai. The rate of corrosion was detected by deep method in 3.5% NaCl solution for 2160 h.

### 3. Results and Discussion

#### 3.1. Functionalisation, Dispersion of FCNT/GO and Curing of Isocyanate

The overall strategy shown in Figure 1 depicts dispersion of active carbon material in isocyanate. The accessible functional groups on the surface of carbon material induce cross-linking to di-isocyanate. Initial reports on a high degree of functionalization followed by fluorination employed to obtain large dispersion and mechanical strength in epoxy nanocomposite [24]. Thereby acid and fluorine covalently bind with active epoxy. Acid functional group readily forms ester while diamine becomes active spacer and readily replace side wall fluorine [24,25]. Here toluene di-isocyanate was employed as an active crosslinking bifunctional spacer between two nano-materials. The induced cross-linking was materialized by excessive probe sonication. The overall challenge of nano particle segregation and constant dispersion in a solvent is overcome by reactive sites both on nanomaterial and diisocyanate precursor.

Structural changes in the composite were noted and analyzed by characteristics IRRA peaks. GO@isocyanate shows specific broad absorption peak at  $3407\text{ cm}^{-1}$  (Figure 2b). While CNT@isocyanate shows relatively small absorbance in the same region (Figure 2a). Separate peaks at  $3298\text{ cm}^{-1}$  and  $3528\text{ cm}^{-1}$  arises in toluene diisocyanate confirms urethane link  $\text{N}=\text{C}$  (Figure 2a). While broad absorbance at  $3400\text{ cm}^{-1}$  is completely absent in the pure toluene di-isocyanate. In pure toluene di-isocyanate, C-H stretching absorption spectra was observed at  $2987\text{ cm}^{-1}$  further strongly recognized in both composites of GO/FCNT@isocyanate due to the influence of non-stacking with the surface and non-hydrogen bonding. While sharp absorption bands were observed in the fingerprint region whereas for pure toluene di-isocyanate a bundle of peaks was observed in this region. Peaks itself at close to  $1377\text{ cm}^{-1}$  commonly observed in all spectrums explains  $-\text{CH}_3$  group of toluene diisocyanate carries forwarded in composite formation. Aromatic nature of toluene diisocyanate compound confirms by absorption peaks at  $1170\text{ cm}^{-1}$  and  $1534\text{ cm}^{-1}$ . The IR absorption spectra at  $1130\text{ cm}^{-1}$  for GO@isocyanate and  $1164\text{ cm}^{-1}$  for FCNT@isocyanate corresponds to the C-C-O ether linkage. Absorption at  $934\text{ cm}^{-1}$  for the GO@isocyanate and  $927\text{ cm}^{-1}$  for FCNT@isocyanate is C-H stretch vibrations of methylene attributed to at least one aliphatic fragment or center. The broad peak at  $2291\text{ cm}^{-1}$  was observed for the toluene diisocyanate which is specific isocyanate bond confirmation further completely vanish in both GO@isocyanate and FCNT@isocyanate composites. It confirms the purpose of curing the isocyanate by nano-embedded particles like FCNT and GO was successfully achieved. It is evidenced by the IRRA that significant change was observed in IRRA absorption spectra of surface incorporated with active functional nanoparticles and only isocyanate as such.

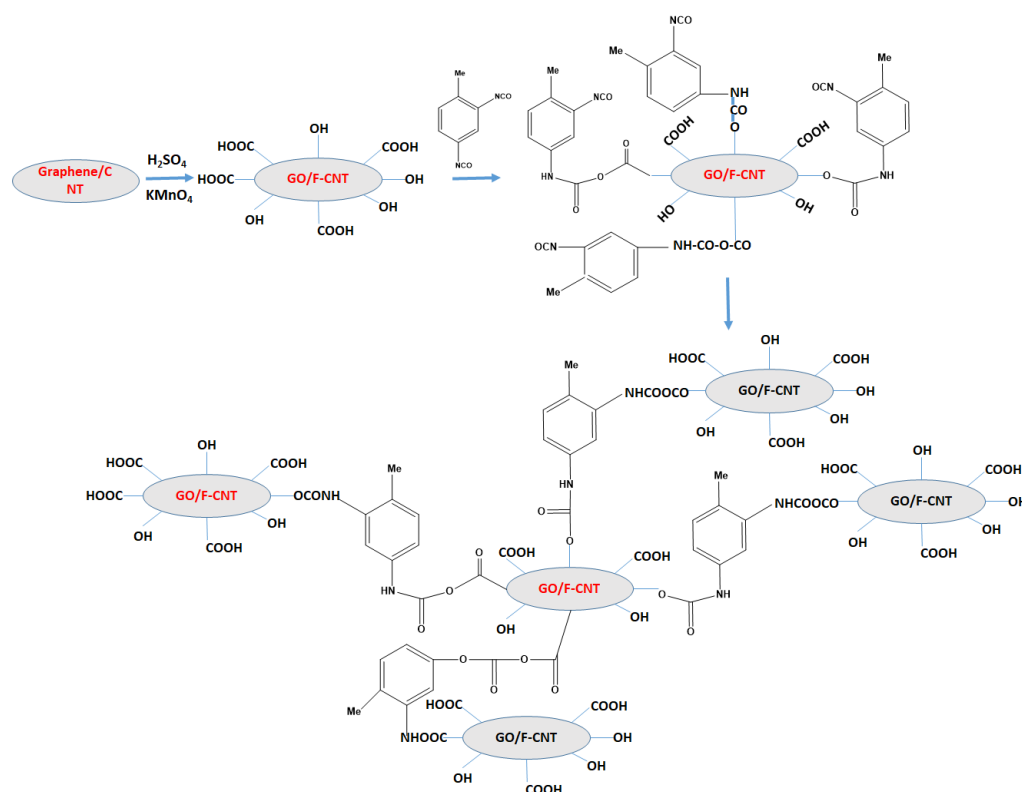


**Figure 1.** Schematic of graphene CNT functionalization, composite formation with toluene diisocyanate.

### 3.2. Interface Chemistry between GO/FCNT@isocyanatematrix

Kozłowski and Jones et al. suggested synergy in two phasic system was owes by interfacial physical  $\pi$ - $\pi$  and covalent chemical compatibility [26,27]. The interfaces of GO/FCNT become more compatible by simultaneously strong covalent and  $\pi$ - $\pi$  interaction with diisocyanate host. While few covalently unbounded GO/FCNT interface has strong  $\pi$ - $\pi$  interaction and remains dispersed without agglomeration (Figure 1). In situ reaction helps in non-agglomeration and phase separation of polymer and GO/FCNT. Hydroxyl and carboxylic acid functional groups grafted onto the GO/FCNT provide a way to in situ chemical integration of the GO/FCNT into the isocyanate system.

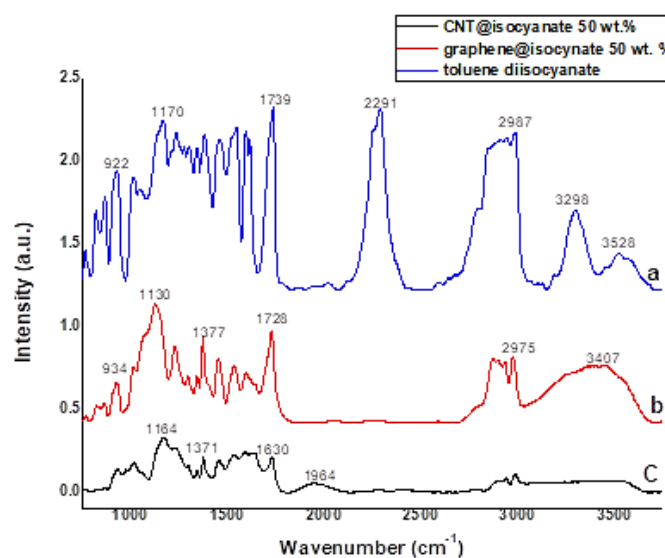


**Figure 2.** IRRA spectra (a) toluene di-isocyanate without doping on steel surface (b) GO@isocyanate 50 wt.% (c) FCNT@isocyanate 50 wt.%.

As mentioned simultaneously strong covalent and  $\pi$ - $\pi$  interaction are involved in facilitating the interfaces between the nanostructured filler and isocyanate matrix. Electron microscopy further corroborates fine dispersion of the nanostructure carbonaceous material in the isocyanate. The properly dispersed GO and MWCNTs over isocyanate in coating is shown by SEM images in Figure 3 on low-alloy steel. The sample was cryo-fractured in liquid nitrogen and cross section SEM image was captured which indicates well dispersed oxidised MWCNTs and GO. There was no clue for the segregation of MWCNTs and GO in SEM somewhere there was hemispherical caps of the MWCNTs was observed. The evidence of covering of polymeric matrix to nanomaterial was also observed in SEM Figure 3a depicts MWCNT@isocyanate while GO@Isocyanate was shown in Figure 3a. The swelling of polymeric matrix observed with nanomaterials and rough surface was observed in coating. Similarly, Figure 3d shows graphene oxide sheets embedded within the isocyanate matrix. The carbon nanomaterial on isocyanate was evaluated with TEM images. The Figure 4a and 4b shows complete dispersion of separated GO sheet and oxidised nanotubes in isocyanate. In Figure 4b TEM of high resolution, it was observed complete covering i.e., wrapping of polymeric matrix to the MWCNTs indicating similar observation of graphene oxide wrapping in isocyanate matrix (Figure 4c). Despite of extensive functionalisation crystalline order of some graphene oxide is preserved shown in Figure 4d in selected area electron diffraction pattern. The sp<sup>2</sup>-hybridized frameworks of graphene oxide and MWCNTs were confirmed by absorption in Raman spectra at 1345 and 1590 cm<sup>-1</sup> of D and G band respectively (Figure 5). It is noted that the positions of D and G bands are finely disturbed while compositing with the isocyanate matrix. While intensity of D and G band are much more affected before and after compositing. In isocyanate matrix intensity of G band was slightly decline rather in MWNTs alone. Further the D band becomes comparable intensive with G band for graphene oxide in isocyanate observing comparable increase in intensity of G band for MWCNTs. As expected after functionalisation intensity of 2D band to be significantly changed in MWCNTs was not observed due to the disruption of p-conjugation arising due to the double bond resonance process which is no more promising for graphene oxide. The compatibility of nanostructure filler and host matrix was owes to the dual modality of covalent bond and  $\pi$ - $\pi$  interactions illustrated in Figures 1, 3 and 5. There are other ways to have compatibility in nanostructure filler and polymeric matrix. To the best of our knowledge and literature references this is sole example for coating application using graphene oxide and oxidised MWCNTs as curing agents.

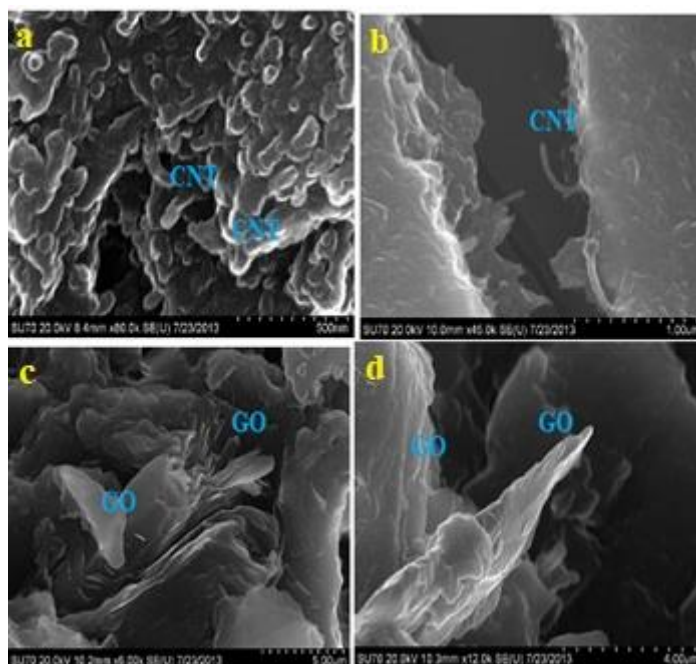


**Figure 3.** Cross section SEM of GO@isocyanate 50 wt.% FCNT@isocyanate 50 wt.%.

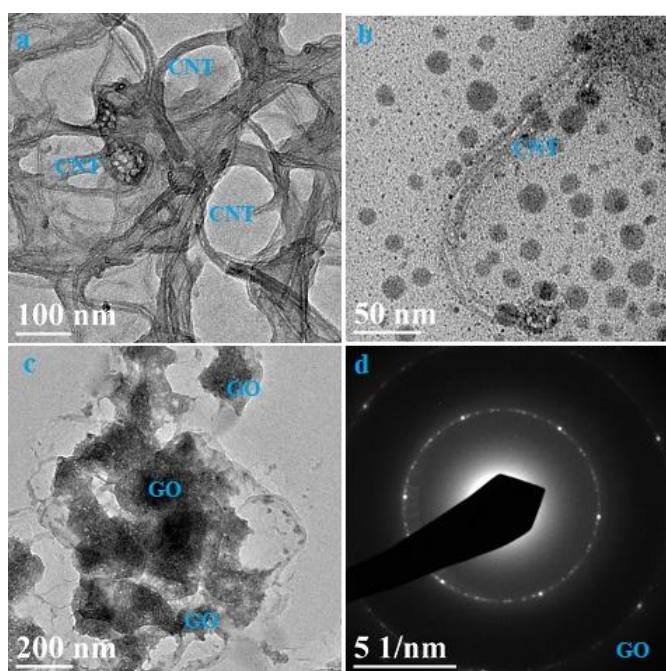


**Figure 4.** TEM of GO@isocyanate 50 wt.% FCNT@isocyanate 50 wt.%. (a–c) and selected area electron diffraction (SAED) pattern acquired for the 50 wt% graphene-oxide@isocyanate composite.

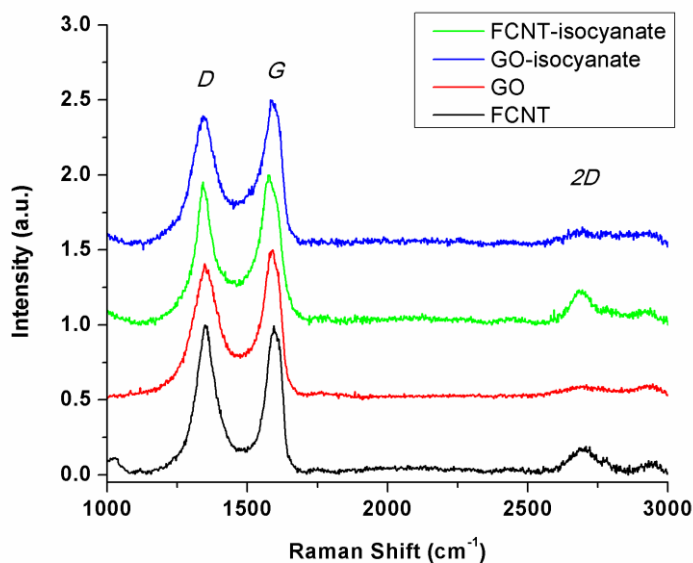


**Figure 5.** Raman spectra of pure GO and FCNT and isocyanate composite with GO and FCNT.

### 3.4. Corrosion Inhibition Endowed by Nanocomposite Coatings

Digital photograph in Figure 6 depicts exposure of 50, 25, 10, and 5 wt.% GO/FCNT@isocyanate in 3.5% NaCl solution for 2160 h. Strong resistance to corrosion observed at higher loading i.e., 25 and 50 wt.% while at 5 and 10 wt.% significant corrosion observed after long exposure to salt solution.

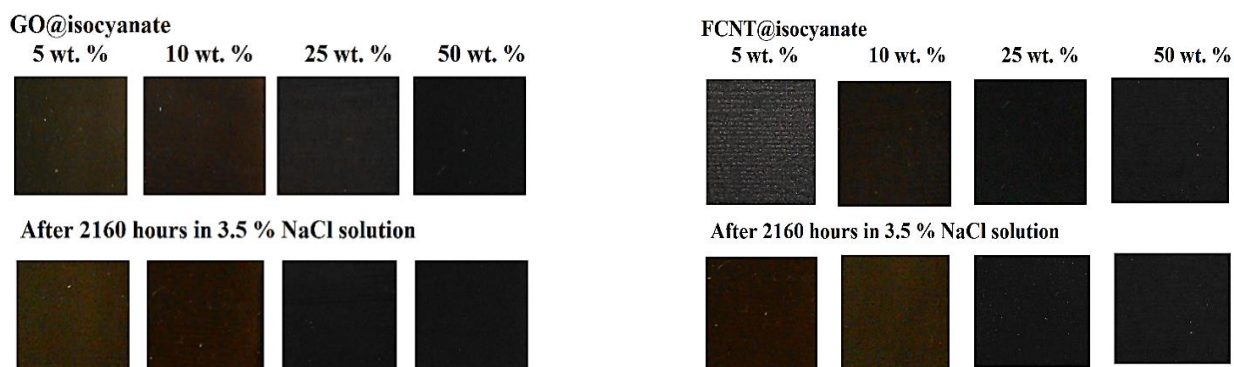


**Figure 6.** Corrosion measurement in salt water (NaCl 3.5%) of GO@isocyanate and FCNT@isocyanate).

### 3.5. Mechanical Properties

Mechanical properties of isocyanate composites have been tested for impact resistance, pencil hardness, scratch hardness, adhesion, cracking resistance and flexibility. The results are summarized in Table 1. It shows the good resistance to cracking (flexibility). The pencil hardness is 5H for all the coating except 5 wt.% GO/FCNT@isocyanate. Similarly, adhesion of coating was fairly good to meet the standards. Adhesion of 5 wt.% GO/FCNT@isocyanate was 4B rest of the coating samples has 5B. Further, all the samples were found to be good resistance over scratch hardness. The average scratch hardness was 2.9 Kg.

**Table 1.** Mechanical properties of polymer films with various %wt of GO/FCNT@isocyanate.

|                       | %Weight of GO/FCNT@isocyanate |      |      |      |                 |      |      |      |
|-----------------------|-------------------------------|------|------|------|-----------------|------|------|------|
|                       | GO@isocyanate                 |      |      |      | FCNT@isocyanate |      |      |      |
|                       | 5                             | 10   | 25   | 50   | 5               | 10   | 25   | 50   |
| Impact Resistance     | Pass                          | Pass | Pass | Pass | Pass            | Pass | Pass | Pass |
| Pencil hardness       | 4H                            | 5H   | 5H   | 5H   | 5H              | 5H   | 5H   | 5H   |
| Flexibility           | Pass                          | Pass | Pass | Pass | Pass            | Pass | Pass | Pass |
| Adhesion              | 3B                            | 5B   | 5B   | 5B   | 5B              | 5B   | 5B   | 5B   |
| Scratch Hardness (Kg) | 2.8                           | 2.9  | 3.0  | 3.0  | 2.8             | 2.9  | 2.9  | 3.0  |

#### 4. Conclusions

A concept of a chemical reaction between two phase materials GO/FCNT with isocyanate executed and utilized as corrosion resistive coating material. Chemically activated carbonaceous nanomaterial was integrated into core structure of polymer matrix united by covalent as well as  $\pi$ - $\pi$  chemical combination. It allows loading about 50 wt.% of nanofiller into polymer matrix delivers better surface and mechanical properties. General problem at high loading of graphene exfoliation and sleeping of nanotubes has been overcome by covalent bonding approach and forms a stable dispersion.

**Acknowledgments:** Vikas Patil is thankful to UGC for Faculty Recharge Program and Start Up grant and INDO-US Science and Technology Forum for Post-Doctoral Visiting Fellowship. We thank group of Prof. Sarabjit Banerjee and Dr. Robert Dennis for analytical support at University at Buffalo.

**Conflicts of Interest:** We confirm that there are no conflicts of interest associated with this publication and there has been no significant financial support for this work that could have influenced its outcome.

#### References

- Shankar, A.R.; Kuma, S.; Piana, F.; Mičušík, M.; Pionteck, J.; Banerjee, S.; Voit, B. Preparation of graphite derivatives by selective reduction of graphite oxide and isocyanate functionalization. *Mater. Chem. Phys.* **2016**, *182*, 237–245.
- Haghdadeh, P.; Ghaffari, M.; Ramezanzadeh, B.; Bahlakeh, G.; Saeb, M.R. Polyurethane coatings reinforced with 3-(triethoxysilyl)propyl isocyanate functionalized graphene oxide nanosheets: Mechanical and anti-corrosion properties. *Prog. Org. Coat.* **2019**, *136*, 105243.
- Maher, M.; Alrashed Mark, D.; Soucek Sadhan, C. Jana Role of graphene oxide and functionalized graphene oxide in protective hybrid coatings. *Prog. Org. Coat.* **2019**, *134*, 197–208.
- Adak, B.; Joshi, M.; Butola, B.S. Polyurethane/functionalized-graphene nanocomposite films with enhanced weather resistance and gas barrier properties. *Compos. Part B Eng.* **2019**, *176*, 107303.
- Stankovich, S.; Piner, R.D.; Nguyen, S.T.; Ruoff, R.S. Synthesis and exfoliation of isocyanate-treated graphene oxide nanoplatelets. *Carbon* **2006**, *44*, 3342–3347.
- Chen, G.; Weng, W.; Wu, D.; Wu, C. PMMA/graphite nanosheets composite and its conducting properties. *Eur. Polym. J.* **2003**, *39*, 2329–2335.
- McLachlan, D.S.; Chiteme, C.; Park, C.; Wise, K.E.; Lowther, S.E.; Lillehei, P.T.; Siochi, E.J.; Harrison, J.S. B AC and DC percolative conductivity of single wall carbon nanotube polymer composites. *J. Polym. Sci.* **2005**, *43*, 3273–3287.
- Berber, S.; Kwon, Y.K.; Tomanek, D. Unusually High Thermal Conductivity of Carbon Nanotubes. *Phys. Rev. Lett.* **2000**, *84*, 4613.
- Lourie, O.; Wagner, H.D. Evaluation of Young's modulus of carbon nanotubes by micro-Raman spectroscopy. *J. Mater. Res.* **1998**, *13*, 2418–2422.
- Walters, D.A.; Ericson, L.M.; Casavant, M.J.; Liu, J.; Colbert, D.T.; Smith, K.A.; Smalley, R.E. Elastic strain of freely suspended single-wall carbon nanotube ropes. *Appl. Phys. Lett.* **1999**, *74*, 3803.
- Andrews, R.; Jacques, D.; Rao, A.M.; Rantell, T.; Derbyshire, F.; Chen, Y.; Chen, J.; Haddon, R.C. Nanotube composite carbon fibers. *Appl. Phys. Lett.* **1999**, *75*, 1329.
- Bansal, A.; Yang, H.; Li, C.; Cho, K.; Benicewicz, B.C.; Kumar, S.K.; Schadler, L.S. Quantitative equivalence between polymer nanocomposites and thin polymer films. *Nat. Mater.* **2005**, *4*, 693–698.
- Schadler, L.S.; Giannaris, S.C.; Ajayan, P.M. Load transfer in carbon nanotube epoxy composites. *Appl. Phys. Lett.* **1998**, *73*, 3842.
- Ajayan, P.; Schadler, L.; Giannaris, C.; Rubio, A. Single-walled carbon nanotube-polymer composites: Strength and weakness. *Adv. Mater.* **2000**, *12*, 750.

15. Sandler, J.; Shaffer, M.S.P.; Prasse, T.; Bauhofer, W.; Schulte, K.; Windle, A.H. Development of a dispersion process for carbon nanotubes in an epoxy matrix and the resulting electrical properties. *Polymer* **1999**, *40*, 5967.
16. Vaccarini, L.; Desarmot, G.; Almairac, R.; Tahir, S.; Goze, C.; Bernier, P. Reinforcement of an epoxy resin by single walled nanotubes. *AIP Conf. Proc.* **2000**, *544*, 521.
17. Gong, X.; Liu, J.; Baskaran, S.; Voise, R.D.; Young, J.S. Surfactant-assisted processing of carbon nanotube/polymer composites. *Chem. Mater.* **2000**, *12*, 1049.
18. Kamae, T.; Drzal, L.T. Carbon fiber/epoxy composite property enhancement through incorporation of carbon nanotubes at the fiber–matrix interphase–Part I: The development of carbon nanotube coated carbon fibers and the evaluation of their adhesion. *Compos. Part A Appl. Sci. Manuf.* **2012**, *43*, 1569–1577.
19. Cui, G.; Bi, Z.; Zhang, R.; Liu, J.; Yu, X.; Li, Z. A comprehensive review on graphene-based anti-corrosive coatings. *Chem. Eng. J.* **2019**, *373*, 104–121.
20. Ding, R.; Chen, S.; Lv, J.; Zhang, W.; Zhao, X.; Liu, J.; Wang, X.; Gui, T.; Li, B.; Tang, Y.; Li, T. W. Study on graphene modified organic anti-corrosion coatings: A comprehensive review. *J. Alloy. Compd.* **2019**, *806*, 611–635.
21. Parhizkar, N.; Shahrabi, T.; Ramezanzadeh, B. Journal of the Synthesis and characterization of a unique isocyanate silane reduced graphene oxide nanosheets; Screening the role of multifunctional nanosheets on the adhesion and corrosion protection performance of an amido-amine cured epoxy composite. *Taiwan Inst. Chem. Eng.* **2018**, *82*, 281–299.
22. Parhizkar, N.; Ramezanzadeh, B.; Shahrabi, T. Corrosion protection and adhesion properties of the epoxy coating applied on the steel substrate pre-treated by a sol-gel based silane coating filled with amino and isocyanate silane functionalized graphene oxide nanosheets. *Appl. Surf. Sci.* **2018**, *439*, 45–59.
23. Patil, V.; Dennis, R.V.; Rout, T.K.; Banerjee, S.; Yadav, G.D. Graphene oxide and functionalized multi walled carbon nanotubes as epoxy curing agents: A novel synthetic approach to nanocomposites containing active nanostructured fillers. *RSC Adv.* **2014**, *4*, 49264–49272.
24. Stevens, J.L.; Huang, A.Y.; Peng, H.; Chiang, I.W.; Khabashesku, V.N.; Margrave, J.L. Sidewall Amino-Functionalization of Single-Walled Carbon Nanotubes through Fluorination and Subsequent Reactions with Terminal Diamines. *Nano Lett.* **2003**, *3*, 331–336.
25. Voevodin, N.N.; Balbyshev, V.N.; Khobaib, M.; Donley, M.S. Nanostructured sol–gel derived conversion coatings based on epoxy-and amino-silanes. *Prog. Org. Coat.* **2003**, *47*, 207–213.
26. Kozłowski, C.; Sherwood, P.M.A. X-ray photoelectron spectroscopic studies of carbon fiber surfaces VIII—A comparison of type I and type II fibers and their interaction with thin resin films. *Carbon* **1987**, *25*, 751–760.
27. Jones, C. The chemistry of carbon fibre surfaces and its effect on interfacial phenomena in fibre/epoxy composites. *Compos. Sci. Technol.* **1991**, *42*, 275–298.